Cellulose fibers deconstruction by twin-screw extrusion with in situ enzymatic hydrolysis via bioextrusion

Gabriel Banvillet, Etienne Gatt, Naceur Belgacem, Julien Bras

Cellulose fibers deconstruction by twin-screw extrusion with *in situ* enzymatic hydrolysis *via* bioextrusion.

Gabriel Banvillet[a,b,1], Etienne Gatt[a,1], Naceur Belgacem[a,c], Julien Bras*[a,c,d]

a. Univ. Grenoble Alpes, CNRS, Grenoble INP (Institute of Engineering Univ. Grenoble Alpes), LGP2, F-38000 Grenoble, France

b. Arjowiggins France SAS, Voiron F-38500, France

c. Institut Universitaire de France (IUF), Paris F-75000, France

d. Nestle Research Center, Lausanne 1100, Switzerland

*Corresponding author: Julien Bras, julien.bras@grenoble-inp.fr

1. Gabriel Banvillet and Etienne Gatt contributed equally to this work.

Abstract

The aim of this work was to study the cellulose fibers deconstruction by twin-screw extrusion with *in situ* enzymatic hydrolysis *via* bioextrusion, for cellulose nanofibrils (CNF) production. Cellulose pulp was extruded with an optimized screw profile, with or without (reference) the addition of an enzymatic solution. An increase of crystallinity index from 67.0% to 73.7% and decrease of DP from 1003 to 419 were observed with bioextrusion. Direct activity measurements of the enzyme confirmed its activity during the process (sugar content increasing from 0.07± 0.004 to 2.38 ± 0.003 mg/mL) and after the process (specific activities around 0.20 CMCU/mL). Enzymes were not deactivated during bioextrusion and

could be recycled. CNF properties were higher with bioextrusion compared to reference (respective quality indices of 55.5 ± 2.7 and 39.8 ± 2.8), with a lower energy consumption. This proof of concept could be optimized for the industrial production of highly concentrated CNF.

Keywords

Cellulose fibers, cellulose nanofibrils, twin-screw extrusion, *in situ* enzymatic hydrolysis, bioextrusion.

1. Introduction

Cellulose fibers have been used since millennia for the production of cotton fabrics in Asia (6000 BC) or the manufacture of the first papers in Egypt (4000 BC). More recent applications were discovered in the 1980's, with the first efficient deconstruction of cellulose fibers into cellulose nanofibrils (Turbak et al., 1983). These cellulose nanofibrils (CNF) have since been proven to be relevant for the substitution of oil-based materials in a wide range of applications, due to their interesting mechanical, optical, barrier and rheological properties. They can be used for energy storage (Kim et al., 2019), barrier layers (Ferrer et al., 2017), pharmaceuticals (Kamel et al., 2020) or as a composite reinforcing phase (Clarkson et al., 2020).

Several pretreatments are used for CNF production, involving chemical or biochemical reactions. Among them, enzymatic hydrolysis is one of the most used due to its easy processing and efficiency (Arantes et al., 2020). Its discovery in 2007 was a major

breakthrough and enabled to drastically reduce the processes energy consumption (Henriksson et al., 2007; Pääkkö et al., 2007). The use of different types of enzymes has been proposed since, such as xylanase (Long et al., 2017) or lytic polysaccharide monooxygenases (Moreau et al., 2019) for example, to improve the pretreatment efficiency. The major asset of this approach is the absence of toxic chemicals, in contrast with pretreatments involving chemical grafting (Rol, Belgacem, et al., 2018). The industrial production of CNF still needs to overcome several drawbacks for their price to be competitive. Among these drawbacks, the low solid content of cellulose pulp during pretreatments and/or mechanical fibrillation processes is predominant, and causes issues for the transport or final use of the material. To solve this issue, the use of twin-screw extruder (TSE) as a mechanical fibrillation process at high solid content has been proposed, as a substitute for conventional processes such as homogenizer, microfluidizer or grinder (Nechyporchuk et al., 2016).

The use of twin-screw extruder for CNF production is a rather recent strategy. Ho et al. (2015) reported the efficient fibrillation of bleached kraft pulp in a twin-screw extruder at high solid content (45 wt%), without any pretreatment of the pulp. The addition of a pretreatment before this mechanical process was proven to have a positive impact on CNF properties and energy consumption, a result observed with enzymatic hydrolysis (Rol et al., 2017), TEMPO-mediated oxidation (Baati et al., 2017; Rol et al., 2017) or phosphorylation (Rol et al., 2019). Twin-screw extrusion is nowadays a feasible process for CNF production, with substantial assets compared to other mechanical fibrillation processes, *i.e.* high solid content, high output and low energy consumption. However, the pretreatments still involve the dilution of the pulp to low solid contents (< 5 wt%), with the addition of a time and energy consuming filtration step to go back to a high solid content before extrusion. High-consistency enzymatic fibrillation is an interesting perspective to overcome this issue

(Kangas et al., 2016; Rahikainen et al., 2020), which has not yet been combined with another fibrillation process.

The combined use of extrusion process and enzymatic hydrolysis for various biomass material deconstruction has been studied for the past two decades (Gatt et al., 2018). Extrusion of lignocellulosic biomass as a pretreatment before fermentation has been proven to greatly increase the cellulose accessibility and glucose yield (Zhang et al., 2012; Zheng et al., 2014). This yield can also be improved by controlling the process temperature (Yoo et al., 2011) or by using alkaline extrusion (Coimbra et al., 2016; Han et al., 2013). Gatt et al. (2019) recently showed that reactive extrusion using enzymes (bioextrusion) led to the improvement of the lignocellulosic biomass hydrolysis at high solid contents (14 - 40 wt%). Several studies have repeatedly shown good *in situ* enzymatic catalysis during the extrusion at high consistencies, on different biomass materials and even with the presence of constraining areas (Duque et al., 2020; Vandenbossche et al., 2014, 2016). However, this bioextrusion strategy has not been applied to the production of CNF (Gatt et al., 2018). Such process could be highly innovative by using the assets of twin-screw extrusion (high solid content, increased output) with an *in situ* enzymatic treatment, while maintaining the high solid content throughout the whole process.

This study aims at investigating the feasibility of *in situ* enzymatic hydrolysis during a twin-screw extrusion process, for cellulose fibers deconstruction into CNF. In this context, a bleached eucalyptus kraft pulp was refined with a Valley beater (80 SR) and processed four times into a laboratory scale twin-screw extruder with an optimized screw profile (Rol, Vergnes, et al., 2020). On one hand, the extrusion was performed with the addition of an aqueous solution of cellulase enzymes. On the other hand, the extrusion was performed

with the addition of an aqueous buffer solution without enzymes, this pulp being used as a reference. Enzymes were efficiently recovered by centrifugation of the pulp, and a carboxymethyl cellulose assay was used (Ghose, 1987) to analyze the influence of the high-shear process on their activity that was not yet proven (Gatt, 2019). Cellulose crystallinity and DP, as well as the production of sugars during the process, were studied. The influence of *in situ* enzymatic hydrolysis on fiber morphology was also investigated by MorFi analysis, optical and scanning electron microscopy. Finally, the mechanical and optical properties of the resulting pulps were determined, in suspension or as films.

2. Experimental section

2.1 Materials

Bleached Eucalyptus Kraft Pulp was purchased as dry pulp sheets from Cenibra, Brazil (Cellulose 83.4 wt%, hemicelluloses 16.2 wt%, lignin 0.4 wt%). Enzyme solution FiberCare© R (Novozyme, Denmark) with an endoglucanase activity of 4770 ECU/g was kindly provided by the company Arjowiggins, France. Chemicals were used as received from suppliers: sodium hydroxide (NaOH 50 % in H_2O, Sigma-Aldrich), acetic acid (CH_3COOH ≥ 99.7 %, Sigma-Aldrich), sodium acetate trihydrate ($CH_3COONa \cdot 3H_2O$ ≥ 99.0 %, Sigma-Aldrich), bis(ethylenediamine)copper(II) hydroxide solution ($Cu(H_2NCH_2CH_2NH_2)_2(OH)_2$ 1.0 M in H_2O, Sigma-Aldrich), 3,5-Dinitrosalicylic acid ($(O_2N)_2C_6H_2$-2-$(OH)CO_2H$, 98 %, Sigma-Aldrich), Potassium sodium tartrate tetrahydrate (KOCOCH(OH)CH(OH)COONa · 4H2O, 99 %, Sigma-Aldrich), total protein kit, micro Lowry, Peterson's modification (Sigma-Aldrich).

2.2 Bioextrusion

2.2.1 Pulp preparation

Cellulose fibers were dispersed in water at room temperature with a laboratory scale pulper for 10 minutes into a 2 wt% suspension. The suspension was refined with a Valley beater (Voith, Germany) until a fibrillation degree of 80 SR as measured with a Shopper Riegler (SR) tester (Paper Testing Association, France) following the ISO 5267-1 standard. This step enables a first weakening of the pulp to avoid clogging at the first pass with the TSE (Rol, Vergnes, et al., 2020). The suspension was then filtered until a concentration of 15 wt% with a nylon sieve of 1 µm mesh size.

2.2.2 Fibrillation by twin-screw extrusion

Bioextrusion was carried out using a twin-screw extruder with a diameter of 16 mm and a length of 640 mm (Thermo Scientific HAAKE Rheomex OS PTW 16 + HAAKE PolyLab OS RheoDrive 7). Screw configuration selected was previously used and described by Rol et al., 2020 (Fig. 1a). This screw profile alternates between conveying elements and mixing areas with reverse elements, to produce shearing forces for cellulose fibrillation. Extrudates were fed with a force feeder (Thermo Scientific, PolyLab OS 567-4002) commonly used in the food industry. A feeding speed of 2 % of the maximal speed was used, leading to an average dry flow of 115 ± 37 g/h. The screw speed was 400 rpm. Temperature was controlled by a cooling system with a setpoint of 10°C, to avoid heating and clogging of pulp due to friction. The pulp underwent 4 passes in total. Due to processing issues, 80 SR cellulose pulp was first hand fed into the extruder at 15 wt% as a pretreatment step (First pass). *In situ* injection of enzyme or buffer solution (reference) was done during the second pass. Third and fourth passes were used to pursue the bioextrusion or the reference treatments. Samples were recovered after each pass, and the associated energy consumptions were calculated with the following equation:

$$\text{Specific Energy Consumption (kWh/t)} = \frac{N \times C \times P_{max}}{N_{max} \times C_{max} \times Q} \quad (1)$$

where N is the screw rotation speed in rpm, N_{max} the maximal rotation speed (1100 rpm), P_{max} the motor maximal power (7 kW), C the measured torque in N.m, C_{max} the maximal torque (130 N.m) and Q the total flow rate in t/h. The specific energy consumption values were cumulated for each pass, and the energy consumption of the refining step was not considered.

2.2.3 *In situ* enzymatic hydrolysis

The pulp underwent a first pass in the twin-screw extruder at 15 wt%, without the addition of any chemical, in order to homogenize pulp pellets and mechanically pretreat the substrate for further processing with the force feeder. A solution of enzymes was injected during the second pass, to assess the efficiency of *in situ* enzymatic hydrolysis. The total contact time between enzymes and pulp was 90 min. A reference sample was produced for comparison, by injecting a buffer solution without enzymes under the same process conditions. The enzyme solution was composed of FiberCare R cellulase and acetate buffer at pH 5.0 (acetic acid and sodium acetate trihydrate). The enzyme concentration of the solution was 10.3 mg/L. The latter was injected from the second module of the extruder using a peristaltic pump (Thermo Scientific) with a flow of 0.25 kg/h. The protein to cellulose ratio was 2 ‰. The dilution induced by the injection of enzyme and reference solutions was compensated by mild pulp drying during process, leading to pulp solid contents of approximatively 20 wt%. The recovered samples were divided in two parts, one for the measurements of cellulase content and activity, the other one for fiber and nanofibrils characterization. For the latter, enzymes were directly deactivated by heating the suspension to 90 °C in a water bath for 5 minutes.

2.3 Cellulase content and activity

2.3.1 Sugars analysis

Pulp samples were diluted with acetate buffer (pH 5.0) in order to reach a solid content of 18 wt% while keeping good pH conditions for the enzymes. They were then centrifuged at 10,000 g for 10 min at 4°C. The reducing sugar content in the supernatants was determined using the 3,5-dinitrosalicylic acid (DNS) method (Miller, 1959). This method titrates all the reducing functions of the different sugars in solution (e.g. oligosaccharides, pentoses, hexoses etc.). All determinations were carried out in triplicate.

2.3.2 Protein analysis

Protein content was measured using a total protein kit, micro Lowry, Peterson's modification (Peterson, 1977). Measurements were conducted on liquid supernatants of extrudates after centrifugation, and all determinations were carried out in duplicate.

2.3.3 Cellulase activity measurements

Cellulase activity measurements were done using the carboxymethyl cellulase assay according to Ghose (1987). Minimum protein concentration obtained with bioextrudate supernatants was 0.028 ± 0.001 mg/mL. For practical reasons, further activity measurements were done using 0.5 mL enzymatic solutions at a protein concentration of 0.026 mg/mL. The same level of measured protein concentration allows the comparison of the remaining cellulase activity after the bioextrusion process. All determinations were carried out in triplicate.

2.4 Cellulose fibers and nanofibrils properties

2.4.1 Nanopapers preparation

Nanopapers (60 g/m²) were made by filtration with a Rapid Köthen sheet former. 2 g of CNF were dispersed to 0.5 wt% with deionized water, followed by 1 min of homogenization with an Ultra Turrax T-25 disperser (IKA, Germany) at 8,000 rpm. Nanopapers were formed by filtrating the suspension under a vacuum of – 500 mbar, the sheet former being equipped with an additional nylon sieve of 1 µm mesh size. The CNF sheets were further dried between two nylon sieves under vacuum at 85 °C for 20 min. Three nanopapers were made for each CNF suspension. Before characterization, the nanopapers were stored in a conditioned room at 23 °C and 50 % RH for 48 h.

2.4.2 MorFi analysis

The analysis of fiber morphology was carried out with the image acquisition system MorFi LB-01 fiber analyzer (Techpap, France). 300 mg of pulp were dispersed in 7 L of water with constant recirculation in the apparatus. The fiber / fine limit was set to 200 µm in length, and the number of analyzed fibers was set to 5,000. The resolution of the MorFi is estimated to be around 5 µm. Two analyses were done on each sample, and average fiber length (µm) and fine content (% in area) were determined.

2.4.3 Optical microscopy

Optical microscopy images were taken with a microscope Axio Imager M1 (Carl Zeiss, Germany) equipped with an AxioCam MRc 5 digital camera. Suspensions were diluted to 0.1 wt% and homogenized for 1 min with an Ultra Turrax T-25 disperser at 8,000 rpm before slide preparation. Magnifications of 50 and 100 times were used, at least 8 images were taken for each magnification and the most representative are presented.

2.4.4 Degree of polymerization

The degree of polymerization (DP) was measured with the ISO 5351:2010 standard. Fibers were dissolved in a bis(ethylenediamine)copper(II) hydroxide solution, and a capillary viscometer was used to determine the intrinsic viscosity [η] in mL/g. The viscosity average DP_v was calculated using the Mark-Houwink-Sakurada equation:

$$\mathrm{DP_v}^{0.905} = 0.75 \times [\eta] \qquad (2)$$

An average DP value was calculated from triplicates.

2.4.5 X-ray diffraction

X-ray diffraction (XRD) was performed on samples under the form of nanopapers deposited on a zero-background Si substrate. An amorphous reference (powder form) was produced by cryocrushing 1 g of raw eucalyptus fibers for 20 minutes at an oscillation frequency of 30 Hz, with 2 zirconium balls in a 20 mL chamber cooled with liquid nitrogen. A diffractometer X'Pert Pro MPD (PANalytical, Netherlands) was used, equipped with a Bragg-Brentano geometry and a copper anode (Kα λ = 1.5419 Å). The angle 2θ ranged from 6° to 60° with a 0.05° interval. The crystallinity index was calculated by amorphous subtraction with the following formula (Foster et al., 2018):

$$\mathrm{CI}\ (\%) = \frac{\mathrm{A_c}}{\mathrm{A_c}+\mathrm{A_a}} \times 100 \qquad (3)$$

where A_c corresponds to the crystalline area of the XRD pattern, and A_a to the amorphous area of the XRD pattern (amorphous reference). The crystalline area is therefore obtained by subtracting the area of the amorphous reference to the area of the sample's total XRD pattern.

2.4.6 Turbidity

Turbidity was measured with a turbidity meter AL-250 (Aqualytic, Germany) on 0.1 wt% suspensions homogenized for 1 min with an Ultra Turrax T-25 disperser at 8,000 rpm. The test measures the scattered light at 90° from an incident light (λ = 860 nm), and the values in Nephelometric Turbidity Units (NTU) are related to the size and shape of the cellulosic fibrous elements of the suspension. Nine measurements were done for each sample and the average value was calculated.

2.4.7 Transmittance

The transmittance of samples in the form of nanopapers was measured with a UV-spectrophotometer (Shimadzu Manufacturing, USA) in photometric mode at a wavelength of 550 nm. Three measurements were done on each nanopaper, 3 nanopapers were analyzed for each sample leading to 9 measurements in total, and the average transmittance value was calculated.

2.4.8 Tear resistance

Tear resistance of nanopapers was measured with a tear tester equipped with a 4000 mN pendulum (Noviprofibre, France) in a conditioned room (23 °C and 50 % RH). Samples of 50 × 65 mm² were pre-cut, and the force (in mN) to complete the propagation of the cut was measured. Three measurements were done on each nanopaper, 3 nanopapers were analyzed for each sample leading to a total of 9 measurements, and the average value was calculated.

2.4.9 Tensile test

Tensile properties of nanopapers were measured in a conditioned room (23 °C and 50 % RH), with a dual column testing system 5965 of 50 kN maximum force (Instron, USA), following

246 the NF Q03-004 standard. 15 × 100 mm² samples were tested with a tensile speed of 10
247 mm/min. The Young's modulus of each sample was calculated using the thickness values of
248 the nanopaper as measured for porosity. Three measurements were done on each
249 nanopaper, 3 nanopapers were analyzed for each sample leading to 9 measurements in
250 total, and the average value was calculated.

251 2.4.10 Porosity

252 Nanopapers were stored 48 h in a conditioned room (23 °C and 50 % RH) and weighted for
253 basis weight calculation. A Lhomargy micrometer was used to measure thickness at 8
254 different positions on the nanopaper, and an average value was calculated. The porosity of
255 the nanopaper (%) was then calculated using the following formula:

256 $$\text{Porosity} = 1 - \frac{\text{BW}}{\text{e} \times \rho_c} \times 100 \qquad (4)$$

257 where BW is the basis weight (kg/m²), e the thickness (m) and ρ_c the density of cellulose
258 (1540 kg/m^3).

259 2.4.11 Quality index

260 A quality index, adapted from the publication of Desmaisons et al., 2017, was used for the
261 comparison of CNF suspensions together. This value regroups 5 tests assessing CNF optical
262 and mechanical properties (turbidity, transmittance, tear resistance, Young's modulus and
263 porosity), and is representative of the global quality of CNF suspensions. The adapted
264 equation used for quality index calculation was identical to that used by Banvillet et al.,
265 (2021).

266 3. Results and discussion

3.1 Influence of bioextrusion on process parameters

The impact of the addition of enzymes on process parameters during extrusion was first assessed, with the measurement of the torque and dry mass flow of pulp (Fig. 1b). The first pass, corresponding to the extrusion of pulp alone, is associated with a dry mass flow of 0.10 kg/h and a torque of 41 N.m. The addition of a buffer solution during the second pass (reference) leads first to an increase of the flow to a value of 0.17 kg/h, then to a drastic decrease of this value, with a flow of 0.05 kg/h during the fourth pass. The addition of the enzyme solution leads to a similar increase of flow during the second pass, which decreases during the subsequent passes. However, while the tendency is comparable to the reference, the decrease of the flow is less important and the final value of 0.12 kg/h during the fourth pass remains higher than the initial dry mass flow. The effect of the enzyme solution is clearly visible with the evolution of the torque. Thus, just after the addition of the enzymes, a major decrease of the torque is observed down to a limit value of 15 N.m, which remains stable for the subsequent passes. This major decrease is not observed with the reference solution, for which the torque decreases gradually to reach a final value of 21 N.m. These differences of process parameters are a first indicator that enzymes are indeed active during extrusion. The decrease of the torque and relative increase of the dry mass flow are likely due to the decrease of pulp viscosity during enzymatic hydrolysis (Nguyen et al., 2015). This phenomenon has a positive impact on the output and energy consumption, as the torque is taken into account in the calculation of specific energy consumption (equation 1).

3.2 Characterization of enzymatic hydrolysis efficiency

3.2.1 *In situ* activity of enzymes

289 The X-ray diffraction patterns were studied for each sample to determine the evolution of
290 cellulose crystallinity during the process. The XRD pattern after 1 pass was typical of
291 cellulose Iβ crystalline structure, with typical diffraction peaks at 2θ angles of 15.2°, 16.7°,
292 22.6° and 34,7°, corresponding to the $(1\bar{1}0)$, (110), (200) and (004) lattice planes respectively
293 (French, 2014; Park et al., 2010). With the addition of the reference solution, further passes
294 through the TSE led to a decrease of the peak intensities, while maintaining the same
295 cellulose Iβ structure. With the addition of the enzyme solution, an increase of peak
296 intensities was observed during the second and following passes. For this sample, the
297 cellulose Iβ structure was also maintained. This increase is therefore due to the enzymatic
298 hydrolysis, which occurs preferentially on disordered cellulose (Bansal et al., 2009). The
299 resulting samples contain a relative higher amount of crystalline cellulose, leading to a
300 globally higher crystallinity.

301 The crystallinity index (CI) was calculated with the XRD patterns of the sample and
302 amorphous cellulose by amorphous subtraction (Fig. 2). This method was used for an
303 optimal accuracy, as the peak height method tends to lead to overestimated values
304 (Ahvenainen et al., 2016; Park et al., 2010). The TSE process alone, with the addition of
305 reference solution, leads to a progressive decrease of CI from 70.4 % to 59.3 %, which
306 remains stable at high energy consumptions. This effect has been widely described for TSE
307 (Ho et al., 2015; Rol et al., 2017) and mechanical fibrillation processes in general, and is due
308 to the partial destruction of the cellulose crystalline structure under high shear. This also
309 leads to a progressive decrease of degree of polymerization (Fig. 2), due to the degradation
310 of cellulose chains (Rol, Banvillet, et al., 2018). The initial degree of polymerization (DP) of
311 1086 decreases therefore linearly until a value of 853, associated with a high energy
312 consumption (26.6 MWh/t).

313 The addition of enzymes, however, drastically changes the crystalline structure of the pulp.
314 The CI shifts from 67.0 % to 73.7 % after the addition of enzymes, with a low increase of
315 energy consumption from 7.9 to 9.8 MWh/t. This value stabilizes and decreases during the
316 subsequent passes, until a final CI of 70.2 % associated with an energy consumption of 14.3
317 MWh/t. The effect of enzymes is also clearly visible on the evolution of DP (Fig. 2), with a
318 brutal decrease from 1003 to 419. It should be noted that the DP decrease observed here (-
319 58 %) is in the same order of magnitude or higher than the DP decrease observed with the
320 use of endoglucanases in dilute conditions. This decrease can range from - 25 % (Hu et al.,
321 2018) to - 65 % (Henriksson et al., 2007) depending on the cellulose source and enzyme
322 dosage. The DP stabilizes and slightly decreases with further passes through the TSE, until a
323 final value of 368. The brutal increase of CI and decrease of DP both confirm the efficiency of
324 enzymes on the 15 wt% solid content pulp. The enzymes cause a decrease of the length of
325 cellulose chains by hydrolysis, and the partial removal of disordered cellulose leading to a
326 higher crystallinity. However, the rapid DP stabilization underlines an important hydrolysis
327 kinetics for the first pass with enzymes, which decreases for subsequent passes. This is
328 possibly due to poor mobility of proteins once dispersed in the pulp, due to its high solid
329 content (Gatt et al., 2018). The evolution of cellulose crystallinity also confirms this
330 hypothesis. For the last two passes with enzymes, the negative effect of the process on
331 cellulose crystalline structure becomes prominent again, causing a decrease of the CI.

332 The activity of enzymes was assessed by recovering the supernatant of the extruded pulp
333 after centrifugation. The measured reducing sugar content in the supernatant demonstrates
334 the existing *in situ* enzymatic activity during bioextrusion (Fig. 3). The value obtained without
335 enzymes (pass 1) shows that the physical constraint itself (thermal and mechanical) is not
336 sufficient for reducing sugar production. The presence of enzymes is therefore mandatory

for this sugar production, as reported by (Gatt et al., 2019). The increasing sugar content with the increasing number of passes underlines the conservation of this activity throughout the process.

3.2.2 *Ex situ* activity of enzymes

Maintained activity was furthermore proved by the direct measurement of cellulase *ex situ* activities with a carboxymethyl cellulase assay (Fig. 3). The initial activity of 0.10 CMCU/mL for FiberCare alone shifts to values between 0.17 and 0.24 CMCU/mL depending on the number of passes through the TSE. Despite the high solid content of 15 wt% and shear rate of 215 s^{-1} (Rol, Vergnes, et al., 2020), these results indicate that the free proteins are still active. Post-extrusion slightly higher results could be due to more accessible cellulose fragments produced during bioextrusion and mixed in the supernatants with remaining proteins. These sugars are not part of the CMC substrate solution during the measurement of cellulase activity. It has to be underlined that post-extrusion activities are not significantly different for each pass, considering the standard deviations. Two different hypothesis can be drawn from that observation. First, the physical constraints of the extrusion process do not appear to deactivate the free remaining cellulases, even when repeated. Then, the increasing sugar content after the second or the third pass might also contribute to a higher content of more accessible cellulose fragments, thus falsely increasing the corresponding enzymatic activity.

The remaining protein contents into the bioextrudate supernatants were also measured, with values of 4.3×10^{-2}, 2.8×10^{-2} and 3.0×10^{-2} mg/mL after 2, 3 and 4 passes with enzymes, respectively. These values are a significant proof that it is possible to recover these enzymes after the extrusion with a simple procedure, even though the complex process

conditions (high solid content and mechanical constraints). Furthermore, these enzymes being active, it would be possible to recycle them and, for example, reduce the amount of required enzymes for a new process. However, there is a clear loss of most of the enzymes at the end of the process, worsened by its repetition. A third of the recovered enzymes in the first bioextrusion pass (pass 2) are lost after the following pass (pass 3). Rates of recovery would probably be improved by a washing and filtration step.

3.3 Cellulose fibers and nanofibrils properties

3.3.1 Morphological properties

A quantitative analysis of the fibers morphological changes was realized with a MorFi tool (Fig. 4). On one hand, the creation of fine elements (length < 200 µm) due to extrusion is visible with the major increase of fine content after 4 passes, from 7.2 % (starting pulp) to 54.0 and 49.5 % for reference and enzyme solutions, respectively. On the other hand, the average fiber length decreases rapidly, from 538 µm (starting pulp) to 310 and 334 µm for reference and enzyme solutions, respectively. These values quantitatively indicate the fiber cutting and fiber deconstruction into micro-scale elements due to the high mechanical constraints of the process. However, this analysis does not show any difference between the reference and bioextrusion. In contrast, optical microscopy images reveal several differences in the fiber and fine elements morphology depending on the treatment. For the reference solution, the number of aggregates increases with fibers deconstruction in the process. These aggregates of fiber fragments and cellulose microfibrils are detected as fine elements by the MorFi analysis, but lead to a poor homogeneity of the suspension. This relative heterogeneity is expected to have a negative impact on the mechanical properties, as these aggregates can increase the number and the size of pores in the nanopapers and act as

fracture-initiating points (Siró et al., 2011). In contrast, the enzyme solution does not lead to fiber aggregation, and the fine elements are more evenly dispersed. This relative homogeneity indicates the efficiency of enzymatic hydrolysis and its positive impact on the presence of aggregates. The enzymatically weakened pulp seems to be more easily and evenly deconstructed by the TSE. In both cases, residual fibers or fiber fragments are present in the pulp, and negatively affect its mechanical and optical properties. These observations were confirmed by SEM pictures. Aggregates obtained with the reference solution were found to be composed of destroyed fibers and CNF bound together during extrusion, which cannot be easily dispersed even after Ultra Turrax mixing. Such aggregates were absent of the sample treated with the enzyme solution. For both samples, the presence of fibers, fiber fragments, and networks of cellulose micro- and nanofibrils was observed.

3.3.2 Mechanical and optical properties

The mechanical and optical properties of the different samples are reported in Table 1. Initial refined pulp at 80 SR has a relatively low turbidity (272 NTU) due to well-individualized fibers and the absence of aggregates. On one hand, the size of the fibers and the resulting large pores in the paper lead to a low transmittance (1.24 %). On the other hand, the mechanical properties of the paper are high (376 mN and 7.33 GPa for tear resistance and Young's modulus, respectively) due to the intact fibers reinforced by external fibrillation. The TSE with reference solution leads to a considerable loss of all properties. This effect has been described in the literature (Ho et al., 2015) and results from the destruction of the cellulose and fiber structure previously observed (CI, DP and morphology). The increase of turbidity to a value of 790 NTU and porosity to a value of 62.0 % are due to the important number of aggregates caused by extrusion, as observed with optical and scanning electron microscopy.

406 Such aggregates also lead to a drastic decrease of transmittance (0.51 %), caused by the
407 heterogeneity of the sample. Furthermore, low Young's modulus (4.17 GPa) indicates that
408 fibers are indeed weakened during the process without the creation of a reinforcing CNF
409 network. Further passes lead to unchanged or worsened (*e.g.* turbidity, Young's modulus
410 and porosity after 4 passes) material properties compared to the reference.

411 The bioextrusion leads to significant differences of pulp properties. After one pass with
412 enzymes (second pass), the transmittance increases to a value of 3.00 % and tear resistance
413 decreases to a value of 72 mN, which shows an effective fiber cutting and creation of fine
414 elements. However, the turbidity (588 NTU), porosity (52.1 %) and Young's modulus (6.24
415 GPa) are negatively affected. These values confirm the aggregation phenomenon with the
416 enzyme solution, although less important than with the reference solution. Further passes
417 lead to a final value of 5.96 % for transmittance, 42 mN for tear resistance, and 7.48 GPa for
418 Young's modulus, the latter being comparable to the starting pulp. Turbidity and porosity
419 remain high (525 NTU and 47.4 % respectively), due to the aggregates and fiber fragments
420 present in the sample.

421 The evolution of quality index as a function of specific energy consumption shows a clear
422 difference in the pulp properties for the bioextrusion compared to the reference (Fig. 5). The
423 first pass without any treatment leads to a quality index of 24.6. With the use of reference
424 solution, the mild fibrillation during the process does not compensate the loss of mechanical
425 and optical properties, for a final quality index of 39.8 and energy consumption of 26.6
426 MWh/t. The addition of enzymes leads to a significant increase of quality index to 45.7, and
427 the final quality index (55.5) is obtained for a lower energy consumption, 14.3 MWh/t.

Latter quality index places the bioextrudated sample among the low grades commercially available CNF (Desmaisons et al., 2017). Globally, its properties are significantly lower than those from recent literature. With an enzymatic pretreatment in dilute conditions, porosities lower than 20 % and Young's moduli between 8 and 15 GPa are usually obtained depending on the fibrillation process (Benítez & Walther, 2017). These results underline that the bioextrusion process presented here is not yet optimized for CNF production, as (i) the extrusion process itself causes a destruction of the cellulose structure and a global fiber weakening, (ii) the CNF network takes time to be created which does not compensate the mechanical and optical properties loss, and (iii) the aggregation of fiber fragments and CNF during extrusion has a negative effect on the pulp homogeneity, even though this aggregation was reduced with the use of enzymes. The energy consumption remains higher than the target for industrial CNF production, which is nowadays around 3 MWh/t with optimized processes like refining (Assis et al., 2018). However, a large part of this energy consumption is due to the first pass without any treatment, which could be removed by a direct addition of enzymes. It should be noted that the cumulative energy consumption of the 3 passes with enzyme solution only is 6.4 MWh/t. With an optimization of the screw profile and process conditions (enzyme/cellulose ratio, pulp solid content, enzyme type), this energy consumption could be reduced even more. The resulting high solid content pulp could be of great interest for applications like molding (Rol, Billot, et al., 2020), while improving the process ease and decreasing the transport costs.

4. Conclusions

This work proves the feasibility of CNF production with bioextrusion. Enzyme *in situ* activity was proven, with a soluble sugar production, drastic increase of CI, decrease of DP and

positive effect on process parameters. Bioextrusion led to the production of CNF with less or no fiber aggregation, resulting in better properties. Furthermore, enzymes were recovered in the bioextrudates by centrifugation. Despite the harsh process conditions, they were proven to be still active. These results open the possibility to recycle enzymes after bioextrusion processes. The high solid content throughout the whole process is a major asset for coating or molding applications.

Acknowledgments

The authors gratefully thank the Association Nationale Recherche Technologie (ANRT) and Arjowiggins France SAS for financial and material support for the PhD thesis. LGP2 is part of the LabEx Tec 21 (Investissements d'Avenir - grant agreement n°ANR-11-LABX-0030) and of PolyNat Carnot Institute (Investissements d'Avenir - grant agreement n° ANR-16-CARN-0025-01). This research was made possible thanks to the facilities of the TekLiCell platform funded by the Région Rhône-Alpes (ERDF: European regional development fund). The authors would like to thank Thierry Encinas from CMTC - Grenoble for the XRD analysis, and Maxime Terrien from LGP2 for the computer-aided design of the twin-screw extruder.

Appendix

E-supplementary data to this article can be found in online version of the paper.

References

1. Ahvenainen, P., Kontro, I., & Svedström, K. (2016). Comparison of sample crystallinity determination methods by X-ray diffraction for challenging cellulose I materials. *Cellulose*, *23*(2), 1073–1086. https://doi.org/10.1007/s10570-016-0881-6

2. Arantes, V., Dias, I. K. R., Berto, G. L., Pereira, B., Marotti, B. S., & Nogueira, C. F. O. (2020). The current status of the enzyme-mediated isolation and functionalization of nanocelluloses: Production, properties, techno-economics, and opportunities. *Cellulose*. https://doi.org/10.1007/s10570-020-03332-1

3. Assis, C. A. de, Iglesias, M. C., Bilodeau, M., Johnson, D., Phillips, R., Peresin, M. S., Bilek, E. M. (Ted), Rojas, O. J., Venditti, R., & Gonzalez, R. (2018). Cellulose micro- and nanofibrils (CMNF) manufacturing—Financial and risk assessment. *Biofuels, Bioproducts and Biorefining*, *12*(2), 251–264. https://doi.org/10.1002/bbb.1835

4. Baati, R., Magnin, A., & Boufi, S. (2017). High Solid Content Production of Nanofibrillar Cellulose via Continuous Extrusion. *ACS Sustainable Chemistry & Engineering*, *5*(3), 2350–2359. https://doi.org/10.1021/acssuschemeng.6b02673

5. Bansal, P., Hall, M., Realff, M. J., Lee, J. H., & Bommarius, A. S. (2009). Modeling cellulase kinetics on lignocellulosic substrates. *Biotechnology Advances*, *27*(6), 833–848. https://doi.org/10.1016/j.biotechadv.2009.06.005

6. Banvillet, G., Depres, G., Belgacem, N., & Bras, J. (2021). Alkaline treatment combined with enzymatic hydrolysis for efficient cellulose nanofibrils production. *Carbohydrate Polymers*, *255*, 117383. https://doi.org/10.1016/j.carbpol.2020.117383

7. Benítez, A. J., & Walther, A. (2017). Cellulose nanofibril nanopapers and bioinspired nanocomposites: A review to understand the mechanical property space. *Journal of Materials Chemistry A*, *5*(31), 16003–16024. https://doi.org/10.1039/C7TA02006F

8. Clarkson, C. M., Azrak, S. M. E. A., Forti, E. S., Schueneman, G. T., Moon, R. J., & Youngblood, J. P. (2020). Recent Developments in Cellulose Nanomaterial Composites. *Advanced Materials*, 2000718. https://doi.org/10.1002/adma.202000718

9. Coimbra, M. C., Duque, A., Saéz, F., Manzanares, P., Garcia-Cruz, C. H., & Ballesteros, M. (2016). Sugar production from wheat straw biomass by alkaline extrusion and enzymatic hydrolysis. *Renewable Energy*, *86*, 1060–1068. https://doi.org/10.1016/j.renene.2015.09.026

10. Desmaisons, J., Boutonnet, E., Rueff, M., Dufresne, A., & Bras, J. (2017). A new quality index for benchmarking of different cellulose nanofibrils. *Carbohydrate Polymers*, *174*, 318–329. https://doi.org/10.1016/j.carbpol.2017.06.032

11. Duque, A., Doménech, P., Álvarez, C., Ballesteros, M., & Manzanares, P. (2020). Study of the bioprocess conditions to produce bioethanol from barley straw pretreated by combined soda and enzyme-catalyzed extrusion. *Renewable Energy*, *158*, 263–270. https://doi.org/10.1016/j.renene.2020.05.130

12. Ferrer, A., Pal, L., & Hubbe, M. (2017). Nanocellulose in packaging: Advances in barrier layer technologies. *Industrial Crops and Products*, *95*, 574–582. https://doi.org/10.1016/j.indcrop.2016.11.012

13. Foster, E. J., Moon, R. J., Agarwal, U. P., Bortner, M. J., Bras, J., Camarero-Espinosa, S., Chan, K. J., Clift, M. J. D., Cranston, E. D., Eichhorn, S. J., Fox, D. M., Hamad, W. Y., Heux, L., Jean, B., Korey, M., Nieh, W., Ong, K. J., Reid, M. S., Renneckar, S., … Youngblood, J. (2018). Current characterization methods for cellulose nanomaterials. *Chemical Society Reviews*, *47*(8), 2609–2679. https://doi.org/10.1039/C6CS00895J

14. French, A. D. (2014). Idealized powder diffraction patterns for cellulose polymorphs. *Cellulose*, *21*(2), 885–896. https://doi.org/10.1007/s10570-013-0030-4

15. Gatt, E. (2019). *Etude de la déconstruction de résidus agricoles lignocellulosiques par extrusion biocatalytique*. These de doctorat, Toulouse, INPT. http://www.theses.fr/2019INPT0006

16. Gatt, E., Khatri, V., Bley, J., Barnabé, S., Vandenbossche, V., & Beauregard, M. (2019). Enzymatic hydrolysis of corn crop residues with high solid loadings: New insights into the impact of bioextrusion on biomass deconstruction using carbohydrate-binding modules. *Bioresource Technology*, *282*, 398–406. https://doi.org/10.1016/j.biortech.2019.03.045

17. Gatt, E., Rigal, L., & Vandenbossche, V. (2018). Biomass pretreatment with reactive extrusion using enzymes: A review. *Industrial Crops and Products*, *122*, 329–339. https://doi.org/10.1016/j.indcrop.2018.05.069

18. Ghose, T. K. (1987). Measurement of cellulase activities. *Pure and Applied Chemistry*, *59*(2), 257–268. https://doi.org/10.1351/pac198759020257

19. Han, M., Kang, K. E., Kim, Y., & Choi, G.-W. (2013). High efficiency bioethanol production from barley straw using a continuous pretreatment reactor. *Process Biochemistry*, *48*(3), 488–495. https://doi.org/10.1016/j.procbio.2013.01.007

20. Henriksson, M., Henriksson, G., Berglund, L. A., & Lindström, T. (2007). An environmentally friendly method for enzyme-assisted preparation of microfibrillated cellulose (MFC) nanofibers. *European Polymer Journal*, *43*(8), 3434–3441. https://doi.org/10.1016/j.eurpolymj.2007.05.038

21. Ho, T. T. T., Abe, K., Zimmermann, T., & Yano, H. (2015). Nanofibrillation of pulp fibers by twin-screw extrusion. *Cellulose*, *22*(1), 421–433. https://doi.org/10.1007/s10570-014-0518-6

22. Hu, J., Tian, D., Renneckar, S., & Saddler, J. N. (2018). Enzyme mediated nanofibrillation of cellulose by the synergistic actions of an endoglucanase, lytic polysaccharide monooxygenase (LPMO) and xylanase. *Scientific Reports*, *8*(1), 3195. https://doi.org/10.1038/s41598-018-21016-6

23. Kamel, R., El-Wakil, N. A., Dufresne, A., & Elkasabgy, N. A. (2020). Nanocellulose: From an agricultural waste to a valuable pharmaceutical ingredient. *International Journal of Biological Macromolecules*, *163*, 1579–1590. https://doi.org/10.1016/j.ijbiomac.2020.07.242

24. Kangas, H., Pere, J., & Qvintus, P. (2016). High-consistency enzymatic fibrillation (HefCel) – a cost-efficient way to produce cellulose nanofibrils (CNF). *TechConnect Briefs*, *1*(2016), 181–183.

25. Kim, J.-H., Lee, D., Lee, Y.-H., Chen, W., & Lee, S.-Y. (2019). Nanocellulose for Energy Storage Systems: Beyond the Limits of Synthetic Materials. *Advanced Materials*, *31*(20), 1804826. https://doi.org/10.1002/adma.201804826

26. Long, L., Tian, D., Hu, J., Wang, F., & Saddler, J. (2017). A xylanase-aided enzymatic pretreatment facilitates cellulose nanofibrillation. *Bioresource Technology*, *243*, 898–904. https://doi.org/10.1016/j.biortech.2017.07.037

27. Miller, G. L. (1959). Use of Dinitrosalicylic Acid Reagent for Determination of Reducing Sugar. *Analytical Chemistry*, *31*(3), 426–428. https://doi.org/10.1021/ac60147a030

28. Moreau, C., Tapin-Lingua, S., Grisel, S., Gimbert, I., Le Gall, S., Meyer, V., Petit-Conil, M., Berrin, J.-G., Cathala, B., & Villares, A. (2019). Lytic polysaccharide monooxygenases

(LPMOs) facilitate cellulose nanofibrils production. *Biotechnology for Biofuels*, *12*(1), 156. https://doi.org/10.1186/s13068-019-1501-0

29. Nechyporchuk, O., Belgacem, M. N., & Bras, J. (2016). Production of cellulose nanofibrils: A review of recent advances. *Industrial Crops and Products*, *93*(Supplement C), 2–25. https://doi.org/10.1016/j.indcrop.2016.02.016

30. Nguyen, T. C., Anne-Archard, D., & Fillaudeau, L. (2015). Rheology of Lignocellulose Suspensions and Impact of Hydrolysis: A Review. In *Filaments in Bioprocesses* (pp. 325–357). Springer, Cham. https://link.springer.com/chapter/10.1007/10_2015_323

31. Pääkkö, M., Ankerfors, M., Kosonen, H., Nykänen, A., Ahola, S., Österberg, M., Ruokolainen, J., Laine, J., Larsson, P. T., Ikkala, O., & Lindström, T. (2007). Enzymatic Hydrolysis Combined with Mechanical Shearing and High-Pressure Homogenization for Nanoscale Cellulose Fibrils and Strong Gels. *Biomacromolecules*, *8*(6), 1934–1941. https://doi.org/10.1021/bm061215p

32. Park, S., Baker, J. O., Himmel, M. E., Parilla, P. A., & Johnson, D. K. (2010). Cellulose crystallinity index: Measurement techniques and their impact on interpreting cellulase performance. *Biotechnology for Biofuels*, *3*(1), 10. https://doi.org/10.1186/1754-6834-3-10

33. Peterson, G. L. (1977). A simplification of the protein assay method of Lowry et al. Which is more generally applicable. *Analytical Biochemistry*, *83*(2), 346–356. https://doi.org/10.1016/0003-2697(77)90043-4

34. Rahikainen, J., Mattila, O., Maloney, T., Lovikka, V., Kruus, K., Suurnäkki, A., & Grönqvist, S. (2020). High consistency mechano-enzymatic pretreatment for kraft fibres: Effect of treatment consistency on fibre properties. *Cellulose*, *27*(9), 5311–5322. https://doi.org/10.1007/s10570-020-03123-8

588 35. Rol, F., Banvillet, G., Meyer, V., Petit-Conil, M., & Bras, J. (2018). Combination of twin-
589 screw extruder and homogenizer to produce high-quality nanofibrillated cellulose
590 with low energy consumption. *Journal of Materials Science*, *53*(17), 12604–12615.
591 https://doi.org/10.1007/s10853-018-2414-1
592 36. Rol, F., Belgacem, M. N., Gandini, A., & Bras, J. (2018). Recent advances in surface-
593 modified cellulose nanofibrils. *Progress in Polymer Science*.
594 https://doi.org/10.1016/j.progpolymsci.2018.09.002
595 37. Rol, F., Belgacem, N., Meyer, V., Petit-Conil, M., & Bras, J. (2019). Production of fire-
596 retardant phosphorylated cellulose fibrils by twin-screw extrusion with low energy
597 consumption. *Cellulose*. https://doi.org/10.1007/s10570-019-02447-4
598 38. Rol, F., Billot, M., Bolloli, M., Beneventi, D., & Bras, J. (2020). Production of 100%
599 Cellulose Nanofibril Objects Using the Molded Cellulose Process: A Feasibility Study.
600 *Industrial & Engineering Chemistry Research*, *59*(16), 7670–7679.
601 https://doi.org/10.1021/acs.iecr.9b06127
602 39. Rol, F., Karakashov, B., Nechyporchuk, O., Terrien, M., Meyer, V., Dufresne, A., Belgacem,
603 M. N., & Bras, J. (2017). Pilot-Scale Twin Screw Extrusion and Chemical Pretreatment
604 as an Energy-Efficient Method for the Production of Nanofibrillated Cellulose at High
605 Solid Content. *ACS Sustainable Chemistry & Engineering*, *5*(8), 6524–6531.
606 https://doi.org/10.1021/acssuschemeng.7b00630
607 40. Rol, F., Vergnes, B., El Kissi, N., & Bras, J. (2020). Nanocellulose Production by Twin-Screw
608 Extrusion: Simulation of the Screw Profile To Increase the Productivity. *ACS*
609 *Sustainable Chemistry & Engineering*, *8*(1), 50–59.
610 https://doi.org/10.1021/acssuschemeng.9b01913

611 41. Siró, I., Plackett, D., Hedenqvist, M., Ankerfors, M., & Lindström, T. (2011). Highly
612 transparent films from carboxymethylated microfibrillated cellulose: The effect of
613 multiple homogenization steps on key properties. *Journal of Applied Polymer Science*,
614 *119*(5), 2652–2660. https://doi.org/10.1002/app.32831
615 42. Turbak, A. F., Snyder, F. W., & Sandberg, K. R. (1983). Microfibrillated cellulose, a new
616 cellulose product: Properties, uses, and commercial potential. *Journal of Applied*
617 *Polymer Science. Applied Polymer Symposium.*, *37*, 815–827.
618 43. Vandenbossche, V., Brault, J., Hernandez-Melendez, O., Evon, P., Barzana, E., Vilarem, G.,
619 & Rigal, L. (2016). Suitability assessment of a continuous process combining thermo-
620 mechano-chemical and bio-catalytic action in a single pilot-scale twin-screw extruder
621 for six different biomass sources. *Bioresource Technology*, *211*, 146–153.
622 https://doi.org/10.1016/j.biortech.2016.03.072
623 44. Vandenbossche, V., Brault, J., Vilarem, G., Hernández-Meléndez, O., Vivaldo-Lima, E.,
624 Hernández-Luna, M., Barzana, E., Duque, A., Manzanares, P., Ballesteros, M., Mata,
625 J., Castellón, E., & Rigal, L. (2014). A new lignocellulosic biomass deconstruction
626 process combining thermo-mechano chemical action and bio-catalytic enzymatic
627 hydrolysis in a twin-screw extruder. *Industrial Crops and Products*, *55*, 258–266.
628 https://doi.org/10.1016/j.indcrop.2014.02.022
629 45. Yoo, J., Alavi, S., Vadlani, P., & Amanor-Boadu, V. (2011). Thermo-mechanical extrusion
630 pretreatment for conversion of soybean hulls to fermentable sugars. *Bioresource*
631 *Technology*, *102*(16), 7583–7590. https://doi.org/10.1016/j.biortech.2011.04.092
632 46. Zhang, S., Xu, Y., & Hanna, M. A. (2012). Pretreatment of Corn Stover with Twin-Screw
633 Extrusion Followed by Enzymatic Saccharification. *Applied Biochemistry and*
634 *Biotechnology*, *166*(2), 458–469. https://doi.org/10.1007/s12010-011-9441-6

635 47. Zheng, J., Choo, K., Bradt, C., Lehoux, R., & Rehmann, L. (2014). Enzymatic hydrolysis of
636 steam exploded corncob residues after pretreatment in a twin-screw extruder.
637 *Biotechnology Reports*, *3*, 99–107. https://doi.org/10.1016/j.btre.2014.06.008
638

639 Figure captions

640 Fig. 1. (a) screw profile used for the twin-screw extrusion, (b) calculated dry mass flow and
641 measured torque during the extrusion process, as functions of the number of passes through
642 the extruder. The asterisks indicate the first analysis after the addition of enzyme or
643 reference solution. Dashed lines are guides to the eye.

644 Fig. 2. Degree of polymerization and crystallinity index calculated from XRD pattern as
645 functions of the specific energy consumption. The asterisks indicate the first analysis after
646 the addition of enzyme or reference solution.

647 Fig. 3. Sugar content in glucose equivalent concentration and enzymatic activity, as functions
648 of the number of passes through the extruder. The enzyme solution is injected at the
649 beginning of pass 2. The analyses are carried out on the supernatant of bioextrudates after a
650 centrifugation at 10,000 g for 10 min at 4°C. The enzymatic activities are measured for a
651 protein concentration of 0.026 mg/mL.

652 Fig. 4. Fine content and average fiber length obtained with a MorFi analyzer, as functions of
653 the specific energy consumption.

654 Fig. 5. Quality index as a function of the specific energy consumption. The asterisks indicate
655 the first analysis after the addition of enzyme or reference solution. Dashed lines are guides
656 to the eye.

657 Tables and Figures

658

659 Table 1. Optical and mechanical properties of CNF in suspension or as nanopapers, and their

660 associated quality index.

	Turbidity (NTU)	Transmittance (%)	Tear resistance (mN)	Young's modulus (GPa)	Porosity (%)	Quality index
80 SR	272 ± 6.8	1.24 ± 0.24	376 ± 73	7.33 ± 0.71	44.8 ± 8.1	36.9 ± 4.5
1 pass	790 ± 25.9	0.51 ± 0.05	199 ± 23	4.17 ± 0.23	62.0 ± 3.0	24.6 ± 2.9
2 passes reference	771 ± 26.7	0.49 ± 0.01	121 ± 8	3.43 ± 0.16	60.5 ± 2.6	27.4 ± 2.2
3 passes reference	772 ± 25.2	0.59 ± 0.01	97 ± 7	3.69 ± 0.13	57.7 ± 1.9	30.8 ± 1.9
4 passes reference	752 ± 23.5	1.42 ± 0.12	72 ± 4	5.21 ± 0.39	51.2 ± 3.4	39.8 ± 2.8
2 passes enzyme	588 ± 31.9	3.00 ± 0.09	72 ± 8	6.24 ± 0.32	52.1 ± 0.3	45.7 ± 2.1
3 passes enzyme	537 ± 15.7	4.84 ± 0.45	53 ± 9	6.44 ± 1.20	49.4 ± 2.8	50.9 ± 4.5
4 passes enzyme	525 ± 19.6	5.96 ± 0.55	42 ± 8	7.48 ± 0.38	47.4 ± 0.8	55.5 ± 2.7

661

662

(a)

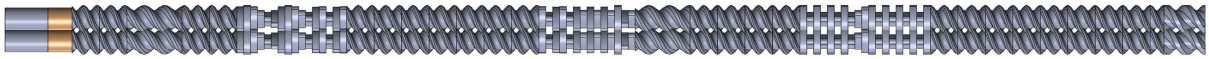

(b)

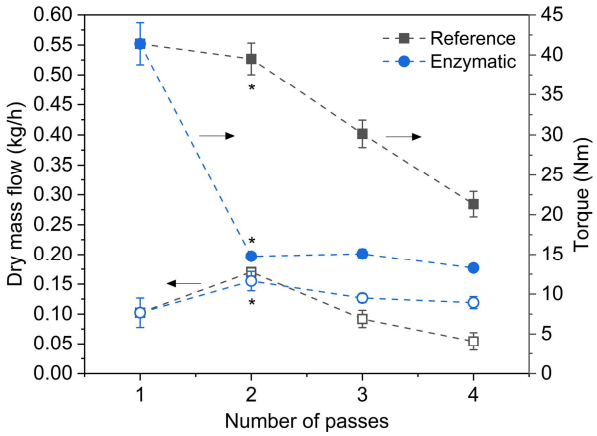

663

664 Fig. 1.

665

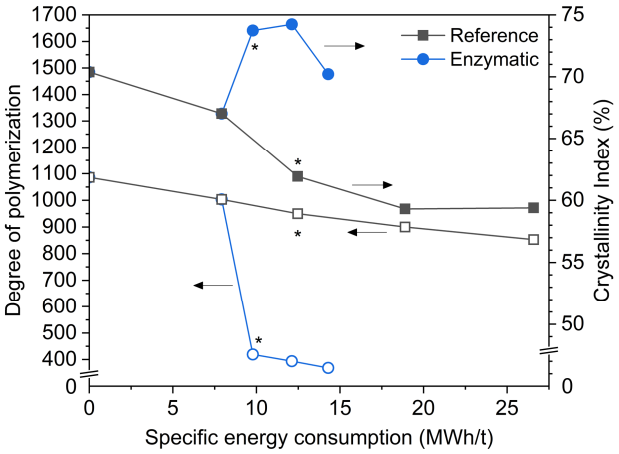
Degree of polymerization
Crystallinity Index (%)
Specific energy consumption (MWh/t)
Reference
Enzymatic
1700
1600
1500
1400
1300
1200
1100
1000
900
800
700
600
500
400
0
75
70
65
60
55
50
0
0
5
10
15
20
25

666

667 Fig. 2.

668

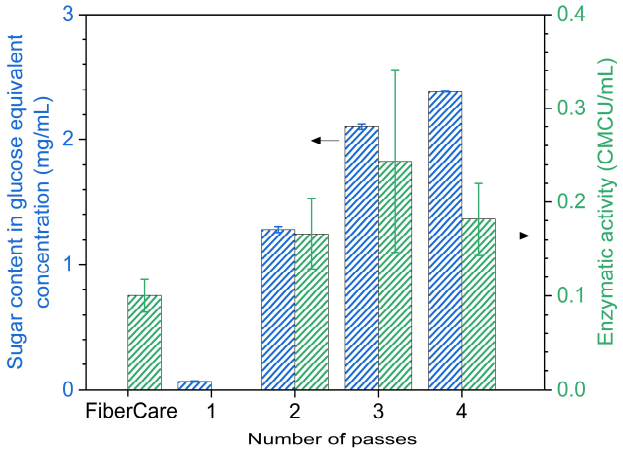
Sugar content in glucose equivalent concentration (mg/mL)
Enzymatic activity (CMCU/mL)
0
1
2
3
0.0
0.1
0.2
0.3
0.4
FiberCare
1
2
3
4
Number of passes

669 Fig. 3.

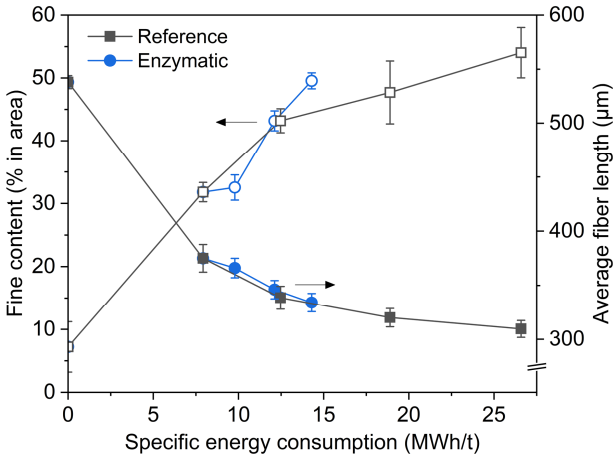
Reference
Enzymatic
Fine content (% in area)
Average fiber length (µm)
Specific energy consumption (MWh/t)
0
10
20
30
40
50
60
300
400
500
600
0
5
10
15
20
25

670

671 Fig. 4.

(b)

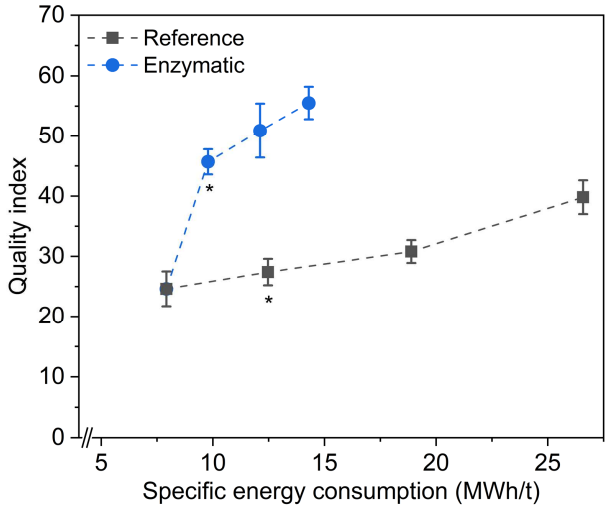

672

673 Fig. 5.

cellulose fibers

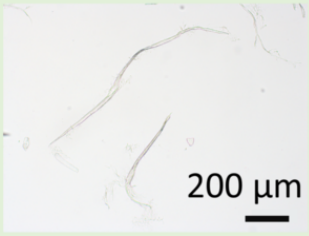

endoglucanase

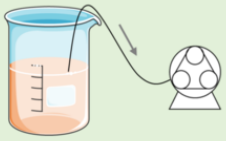

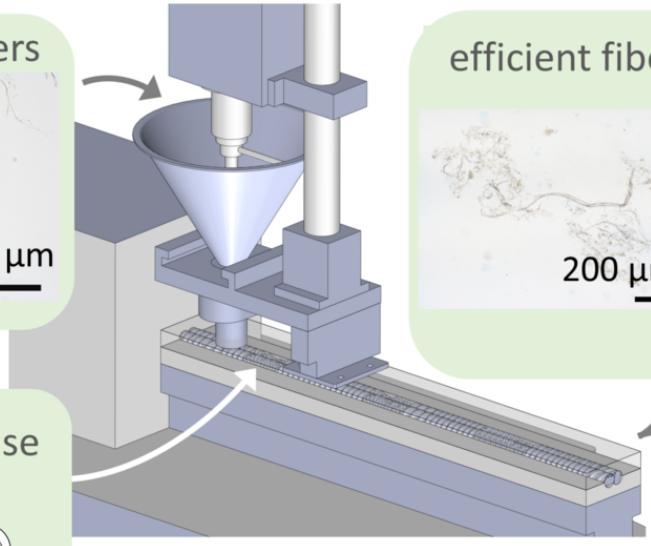

efficient fiber deconstruction

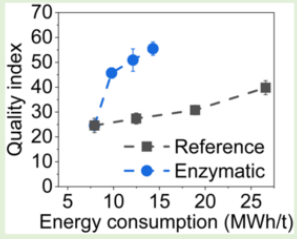

enzymes recovered and still active (0.20 CMCU/mL)